Major and Trace Element Geochemistry of the European Kupferschiefer – An Evaluation of Analytical Techniques

Rahfeld, A.; Wiehl, N.; Dreßler, S.; Möckel, R.; Gutzmer, J.;

Originally published:

March 2018

Geostandards and Geoanalytical Research 18(2018)2, 132-141

DOI: https://doi.org/10.1144/geochem2017-033

Major and Trace Element Geochemistry of the European Kupferschiefer – An Evaluation of Analytical Techniques

Anne Rahfeld[1*], Norbert Wiehl[2], Sandra Dressler[3], Robert Möckel[1], Jens Gutzmer[1]

[1] Helmholtz-Zentrum Dresden-Rossendorf, Helmholtz Institute Freiberg for Resource Technology, 09599 Freiberg, Germany

[2] Institute for Nuclear Chemistry, Johannes Gutenberg University Mainz, 55128 Mainz, Germany

[3] Department of Chemistry, Loughborough University, Loughborough LE11 3TU, United Kingdom

Communication to: a.rahfeld@hzdr.de

Telephone: +49 351 260 3542

Abstract

Simple and rapid techniques are needed for routine quantitative chemical bulk-rock analyses of Kupferschiefer, a black shale containing variable amounts of silicates, base metal sulphides, carbonates and an organic content of up to 30 weight percent. In this study, WD-XRF, TXRF, and ICP-OES of acid- as well as peroxide-digested samples were tested as potential techniques based on their availability and adaptability to analyse major (Si, Ti, Al, Mg, Ca, Fe, K, but also Cu, Zn, Pb) and selected trace (Ag, As, Ba, Co, Mo, Ni, V) element concentrations. Because of the absence of a suitable reference material, a comparative study was undertaken using instrumental neutron activation analysis to ascertain the accuracy of different approaches. Our results suggest that data from ICP-OES were much higher in accuracy compared to INAA than those from WD-XRF and TXRF, independent of the digestion procedure. The choice of digestion procedure is reflected in low detection limits but an underestimation of Cu, Ag, Co, and V

concentrations reported by ICP-OES relative to those obtained by INAA in the case of acid digestion and increased detection limits coupled with a loss of over 25 % Ag relative to INAA for peroxide digestion.

Supplementary material: Geochemical data, List of irradiation times and measured isotopes

Introduction

Whilst a suite of suitable analytical methods is available for quantitative chemical analyses of common silicate rocks (Heinrich and Hermann, 1990), many ores and mineral raw materials impose significant challenges for geochemical analysis. This is especially valid, if a sample consists of complex or refractory minerals with high metal concentrations in combination with silicates and an abundance of organic material. All these attributes are characteristics of the European Kupferschiefer and render quantitative bulk geochemical analyses challenging.

In the strictest sense, the term Kupferschiefer (`copper shale') describes a highly carbonaceous and carbonate-bearing shale that forms the base of the Zechstein sequence developed across Central Europe in an intracontinental sedimentary basin of Permian age (Wedepohl, 1964; Paul, 2006; Borg et al., 2012). Though several lithotypes (carbonaceous shale, sandstone, limestone) host stratabound polymetallic base metal mineralization, it is the Kupferschiefer itself that forms the center of the mineral system (Vaughan et al., 1989; Speczik, 1995; Bechtel et al., 2000; Borg et al., 2012). Today, large-scale industrial exploitation of the Kupferschiefer-type ore deposits takes place in Poland, making the Kupferschiefer-type deposits Europe's largest source of Cu and Ag (KGHM Polska Miedź, 2015; Thomson Reuters, 2015).

45 The highly carbonaceous Kupferschiefer shale contains up to 30 wt% C_{org} (Matlakowska and
46 Sklodowska, 2011). The organic matter is composed primarily of marine kerogen type II with the
47 addition of minor amounts of type III (Sun and Püttmann, 2004), i.e., a mixture of aliphatic and
48 aromatic compounds with a poor reactivity to solvents. The Kupferschiefer also contains very
49 variable concentrations of inorganic carbonate - most commonly represented by the minerals
50 dolomite and calcite – and of clay minerals. The latter are represented by illitic mica, and
51 varying amounts of kaolinite and chlorite (Wedepohl, 1964; Bechtel et al., 2000). The sulfide
52 mineralogy is consistent in its complexity. Whilst Kupferschiefer mineralization comprises
53 predominantly of bornite, chalcocite, digenite, chalcopyrite, non-stoichiometric Cu-sulfides,
54 pyrite, sphalerite, galena, covellite, cobaltite and minerals of the tennantite-tetrahedrite series
55 (Vaughan et al., 1989; Matlakowska et al., 2012) there are more than 80 ore minerals that have
56 been reported to occur in minor and trace amounts (Piestrzynski and Pieczonka, 2012).
57 The combination of organic carbon, silicates, and sulfides present in mineralized Kupferschiefer
58 poses significant difficulties in quantitative chemical bulk analysis. Geochemical studies on
59 carbonaceous shales (Quinby-Hunt et al., 1989; Henrique-Pinto et al., 2017) have obtained
60 accurate results by a combination of instrumental neutron activation analysis (INAA) and
61 multiple-step digestion procedures with ICP-MS. However, this approach is impractical in daily
62 routine analysis. It is thus little surprising that there is very limited bulk geochemical data
63 available for the Kupferschiefer in the published literature. The little geochemical data that is
64 available for the Kupferschiefer has often been collected by stationary or portable XRF for major
65 element and base metal concentrations (Tab. 1). Trace element analysis, excluding Au, Pt, Pd,
66 Re, were commonly obtained by ICP-OES/MS with HF-based digestion procedures (Bechtel et

al., 2001a; Müller et al., 2008). Little is known regarding the errors associated with these analyses, due to the absence of an appropriate reference material.

Table 1: Techniques used in recent studies of base metal concentrations in mineralized Kupferschiefer [1]

INAA	ICP-OES/MS	Portable/stationary XRF	XRF Fusion
Wennrich et al., 1988	Bechtel et al., 2001a; Borg et al., 2005; Müller et al., 2008; Kamradt et al., 2012	Bechtel et al., 2001a, 2001b, 2002; Schubert et al., 2003; Borg et al., 2005; Müller et al., 2008; Oszczepalski et al., 2011; Kamradt et al., 2012	none

[1] Portable and stationary XRF analysis were based on pressed powder tablets

The present study was carried out within the framework of the international EcoMetals research project (Kutschke et al., 2015) with the goal to identify an efficient and robust approach to quantitative chemical analysis of well-mineralized Kupferschiefer. Two types of digestion procedures were tested. Peroxide digestion within an HCl-solution was chosen, based on its recommendation for sulfide and organic-rich materials (Halicz and Russell, 1986; Balcerzak, 2002; Twyman, 2005). The well-established HNO_3-HF-based acid digestion procedure (Hill, 2007) was tested as an alternative. It was decided to use ICP-OES instead of MS due to the fact that the concentration of copper was expected to be in most samples well above 10,000 ppm. In addition, most trace elements of interest (Ag, As, Co, Mo, Ni, V) range well above 100 ppm and do not require a method with detection limits as low as those of ICP-MS. Pressed powder tablets were used for XRF analysis. A preparation of glass beads by fusion was prohibited by standard procedures, owing mainly to the high concentration of sulfide and copper (more detail in the discussion).

Comparative values of a selection of Kupferschiefer samples were collected by INAA – an analytical method based on powder sample and not requiring any reference materials. These data were used to compare the accuracy of ICP-OES and XRF data.

Materials and Methods

Sample Materials

A set of 7 samples was selected to represent Kupferschiefer from different localities in Germany and Poland (Tab. 2). Sample M-KS was collected from a low grade Kupferschiefer surface stockpile (Kamradt et al., 2012) , while W-KS was collected underground at the Wettelrode Fortschritt shaft for this project. Well-mineralized Kupferschiefer samples were further collected at different sites from the Polish Polkowice-Sieroszowice and Rudna mines. In addition, a flotation concentrate from the Lubin concentrator of KGHM (Poland) was included. Although this concentrate originates from a mixture of different mineralized lithotypes (Kupferschiefer-, sandstone- and carbonate-type ores) it was deemed necessary to consider this material as part of this methodological study.

Table 2: List of samples and their respective origin

	Wettelrode	**Mansfeld dump**	**Polkowice**	**Rudna**	**Lubin**
Kupferschiefer samples	W-KS	M-KS	P-KS-2 P-KS-3	R-KS-1 R-KS-2	L-KS-Con*

* flotation concentrate

At least 3kg of each sample were collected and subsequently crushed, milled ≤ to 63µm with a planetary ball mill, dried, and then split following the procedure shown in Fig. 1.

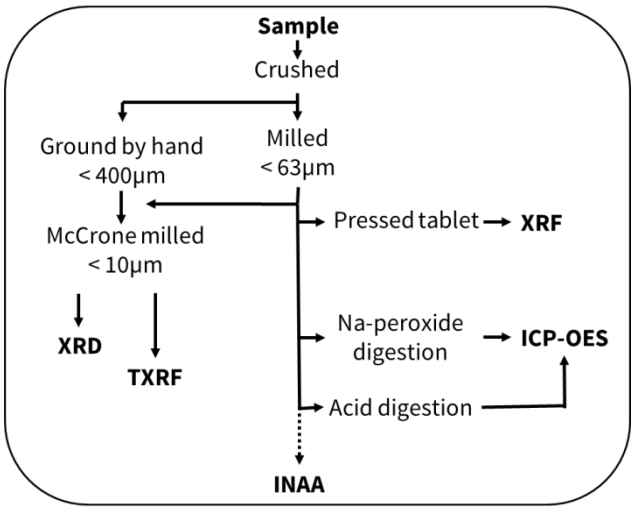

Figure 1: Illustration of the sample treatment and subsequent geochemical and mineralogical analysis

Mineralogical data were gathered using X-ray diffraction (XRD). This mineralogical information was used to correct XRF spectra evaluation by designing a suitable component list, choice of a suitable digestion technique, and validation of the final geochemical results. An overview of the mineralogical composition of all samples is provided in table 3. Details regarding mineralogical studies on this suite of samples are presented in a companion study (Rahfeld et al., submitted 2017).

Table 3: Quantitative mineralogical composition of sample material without organic content by XRD. Values reported in weight percent with a conservatively estimated relative error of 15%. The organic carbon content was determined separately by CNS analysis. (Carbonates: dolomite, ankerite, and calcite; Clays: white mica, kaolinite, and chlorite; Cu-sulfides: chalcocite, bornite, chalcopyrite, covellite; Sulfides: pyrite, galena, and sphalerite)

	Quartz	Carbonates	Clays	Feldspar	Cu-Sulfides	Sulfides	C_{org}
M-KS	18	36	26	9	<2	3	2.2
W-KS	22	8	38	6	5	7	14.4
R-KS-1	11	38	24	5	7	10	7.9
R-KS-2	9	21	40	8	5	7	7.4
P-KS-2	19	38	27	3	8	< 1	7.1
P-KS-3	17	5	32	1	32	< 1	9.3
L-KS-Con	8	13	17	4	25	13	9.1

Reference Materials

At present time, no geological reference material of black shale composition with base metal enrichment above 100 ppm (Kane et al., 1990; Pertov et al., 2007) is available. As alternative reference material IGS-24, supplied by MBH Analytical Ltd, was selected - a cobalt ore with concentrations of Si, Cu, Co and Ni (Lister, 1978) that are similar to those of the Kupferschiefer. However, this reference material does not have the same complex mineralogical composition. To test the effectiveness of the analytical approach used in this study on at least one other black shale, we used the in-house standard SH-1 supplied by the University of Quebec (Henrique-Pinto et al., 2017).

To account for the uncertainty introduced by the lack of a suitable reference material, INAA measurements were carried out. INAA has the advantage that it requires no rock standards, no sample digestion, and still will yield accurate results with a calibration based on single element standards. Uncertainty and bias in INAA is independent of those associated with most other chemical techniques as it depends on nuclear, opposed to atomic, properties of the determined elements (NIST).

Sample digestion for ICP-OES

Two digestion techniques were utilized in the preparation of solutions for ICP-OES analyses. Peroxide digestion (PD), a type of caustic fusion, was carried out in zirconium crucibles using a mixture of 0.5000 g sample material, 6g Na_2O_2, and 1g Na_2CO_3, based on the FluXana operating instruction (FXSOP-0083-01). The digestion was completed with a Vulcan 2-station gas fusion

machine. An adapted fusion program composed of 240 s prefusion (150 m^3/h gas – 20 m^3/h oxygen – 800 m^3/h air) followed by 180 sec fusion (150-20-500) and 180sec cooling was implemented to minimize the explosiveness of the reaction. The prefusion settings produced the smallest possible flame and kept the initially violent reaction of the peroxide with the organic matter well contained. Afterwards, the cooled zirconium crucible was dropped into a beaker with70 ml deionized water (DI-H_2O) and covered by a watch glass. 70 ml 16% HCl was added as soon as the reaction had come to an end, causing a change in the solution color and transparency from turbid to clear. The crucible was removed and cleaned with 16% HCl and deionized H_2O. The remaining solution was boiled for 3 minutes to achieve full dissolution and conversion. Under the addition of DI-H_2O, 200 ml of solution were transferred into a PET bottle using a measuring cylinder.

A second set of solutions was prepared by acid digestion (AD) in glassy carbon vessels. In this approach, 0.1000 g of each sample was dissolved in 50 ml DI-H_2O with an addition of 2.5 ml HNO_3. Samples P-KS-2, P-KS-3, R-KS-2, and W-KS with high TOC contents were treated with 5ml HNO_3 and 3 ml HF overnight and at a temperature of 100°C. Afterwards, the solutions were heated to 50 °C (60 min) and 100°C (30 min) before vaporization. In all four samples a dark residue remained in the solution that was subsequently filtered. Samples M-KS, and R-KS-2 were dissolved in 3ml HNO_3 and 5ml HF. A dark residue remained and required a filtration step.

Inductively coupled plasma optical emission spectroscopy

The ICP-OES measurements were conducted at the Department of Mineralogy at the Technical University Bergakademie Freiberg. Two standard solutions were prepared for calibration. One of

these was composed of Merck multi-element solution number four (ME-IV) containing Ag, Al, As, Ba, Ca, Cu, Co, Fe, K, Mg, Pb, Zn and the other a solution of Mo, V, Sb, Se, Si, Ti . The working solutions were prepared with a dilution factor of 1:100 and 1:10. All ICP-OES measurements were carried out using a Perkin Elmer Optima 3300DV spectrometer and autosampler AS 90. The spectrometer was operated at 1.3 kW, with 0.8 L min^{-1} Ar nebuliser gas, 15.0 L min^{-1} plasma gas and 0.5 L min^{-1} auxiliary gas in cross flow dispersion. As part of ongoing quality control, a blank and a reference material were analyzed with each batch of samples. Every third sample was run in duplicate. The results of the duplicates are reported as averages.

Wavelength-dispersive-X-ray fluorescence spectrometry

For XRF, pressed powder pellets with a diameter of 40 mm were prepared using 10g milled sample material and 2g pure wax (C-wax, $C_{18}H_{36}O_2N_2$). This mixture was homogenized in a mixing mill. The tablets were pressed at 18kN for 30 seconds. The sample material could not be calcined, because temperatures above 780°C led to sintering and prohibited removal of the material from the crucible. Therefore, primary, untreated material was used. Total carbon (TC) data supplied by CNS analyses was used for a correct calculation of element concentrations. All WD-XRF analyses were executed using a PANalytical AxiosMAX spectrometer with 60 kV and a current of 66 mA at lower, 25 kV with 160 mA at higher wavelengths. The spectrometer is equipped with a Rh-anode X-ray tube. The wavelength dispersive system uses five crystals (LiF (2 0 0), Ge (1 1 1), PE (0 0 2), PX1 and LiF (2 2 0)). The Kα lines of Ag, Al, As, Ba, Ca, Cl, Cr, Co, Cu, F, Fe K, Mg, Mn, Na, Ni, P, Rb, Si, Sr, Ti, V, Y, Zn and Lβ line of Pb were selected for the quantification. Quantitative analysis was performed by the PANalytical 'standardless' analytical program *Omnian* (Axios, 2005).

Total reflection X-ray fluorescence spectrometry

A homogenous suspension was prepared by mixing 100 mg of fine powdered sample material with 5 ml of an aqueous 1 vol % Triton X-100 solution (Klockenkämper and Von Bohlen, 2015). For convenience, McCrone milled material with a particle size below 10 µm – identical to that commonly used for quantitative X-ray powder diffraction analysis – was used. 40 µg Bi and 40 µg Y solution were added as internal standards to the suspension. Aliquots of 10 µl were pipetted onto 30 mm quartz-glass carriers and dried. The measurement was completed with a S2 Picofox instrument from Bruker. The air-cooled spectrometer is equipped with a metal ceramic X-ray tube, a Mo-target and a Ni/C-multilayer monochromator. The tube was operated at 50 kV and 600 µA. The measurement itself was completed with a silicon drift detector (SDD) with a resolution of less than 160 eV and the Spectra processing software. Measurements were repeated twice. Reported values are averages.

Instrumental neutron activation analysis (INAA)

A suite of 25 elements was measured by INAA in five of the seven samples considered in this study (Tab. 2). Two hundred milligram of powdered sample material were filled into polyethylene capsules and then irradiated at the University of Mainz TRIGA research reactor with thermal neutrons at 100 kW_{th}. The samples were first irradiated in the pneumatic system of the TRIGA Mainz research reactor in a neutron flux of 1.7e12 n/cm^2 s for 1 min to detect the isotopes with relatively short half-lives (electronic supplement). Three measurements were taken: one immediately after irradiation, a second after about 5 min decay and a third one after

~20 min decay. For isotopes with longer half-lives a second irradiation was performed in the carousel facility for 6h at 0.7e12 n/cm²s. The samples were measured after a week and a month of cooling time. A Ti and Fe standard was measured together with the samples as flux monitor for the pneumatic and carousel measurements.

Samples from the carousel were measured with a high purity germanium detector in 7 cm distance to the detector with less than 3 % dead time. The short-lived isotopes were measured with a high purity germanium detector (HP-Ge) equipped with a loss-free-counting system (LFC, Westphal, 2008) at a distance of 9 and 19 cm to the detector. The measurements were performed and analyzed using the Genie 2000 software, version 3.2 (Copyright Canberra Industries Inc., 2009). Elemental contents were determined relative to single element standards which were irradiated and counted under the same conditions. The measurement uncertainty of the element concentrations were determined based on the relative peak area uncertainty. The Mo concentration was measured by INAA using the 739 keV line of the isotope ^{99}Mo after a week of cooling time. Mo has an increased uncertainty of up to 12 % due to increased peak area uncertainty. The aluminum concentration was calculated from the ^{28}Al activation product. Measurement of a Si standard determined that 1.2 % ^{28}Al is formed in the activation of 100% Si. The average Si content of about 13 wt% in the samples corresponds to an error of 0.1 wt% that was deduced from the calculated Al concentration. Only low or no activity of isotope ^{31}Si could be found to determine the Si concentration in the samples by INAA, due to low gamma-ray intensities and the low neutron capture cross section (Iγ 0.07%) of ^{31}Si. Calculation of Si concentrations based on ^{29}Al did not yield realistic results that could be related to the observed mineralogical composition. To have an alternative estimate of the realistic Si content, Si within

232 the samples was calculated based on quantitative XRD measurements of quartz, clay minerals
233 and feldspar (Tab. 3, Fig. 4).
234
235 **Results obtained for reference materials**
236 IGS-24 was used primarily to compare the performance of the acid (AD) and peroxide digestion
237 (PD) process as applied to a Cu- and Si-rich sample material. Si and Cu were determined with a
238 high accuracy by both OES-PD and XRF. OES-AD underestimated the Cu content by about 14 %.
239 Peroxide digestion had an overall higher accuracy with an average deviation of only 6.5 and 7.7
240 % in major and trace elements compared to 14.7 and 11.9% in acid digested samples measured
241 by ICP-OES (Fig. 2). In particular, Al, Co, and Ni could be detected with a lower deviation to the
242 standard. Co was underestimated with all three techniques, whereby OES-PD showed the best
243 performance. SH-1 (Fig. 2) was digested with peroxide to test specifically the suitability of this
244 procedure for black shales. No results regarding the base metals are available, since their
245 concentration in this reference sample is below the detection limit of the analytical methods
246 used. OES-PD has an average deviation from the in-house standard by 5.9 %, while XRF has an
247 increased deviation from the standard of 13 %. Both OES-PD and XRF underestimated the Si
248 content by about 8%. Results with high accuracy (< 5 % deviation) were obtained for Al, Ba, Fe,
249 Mg, and V using OES-PD.

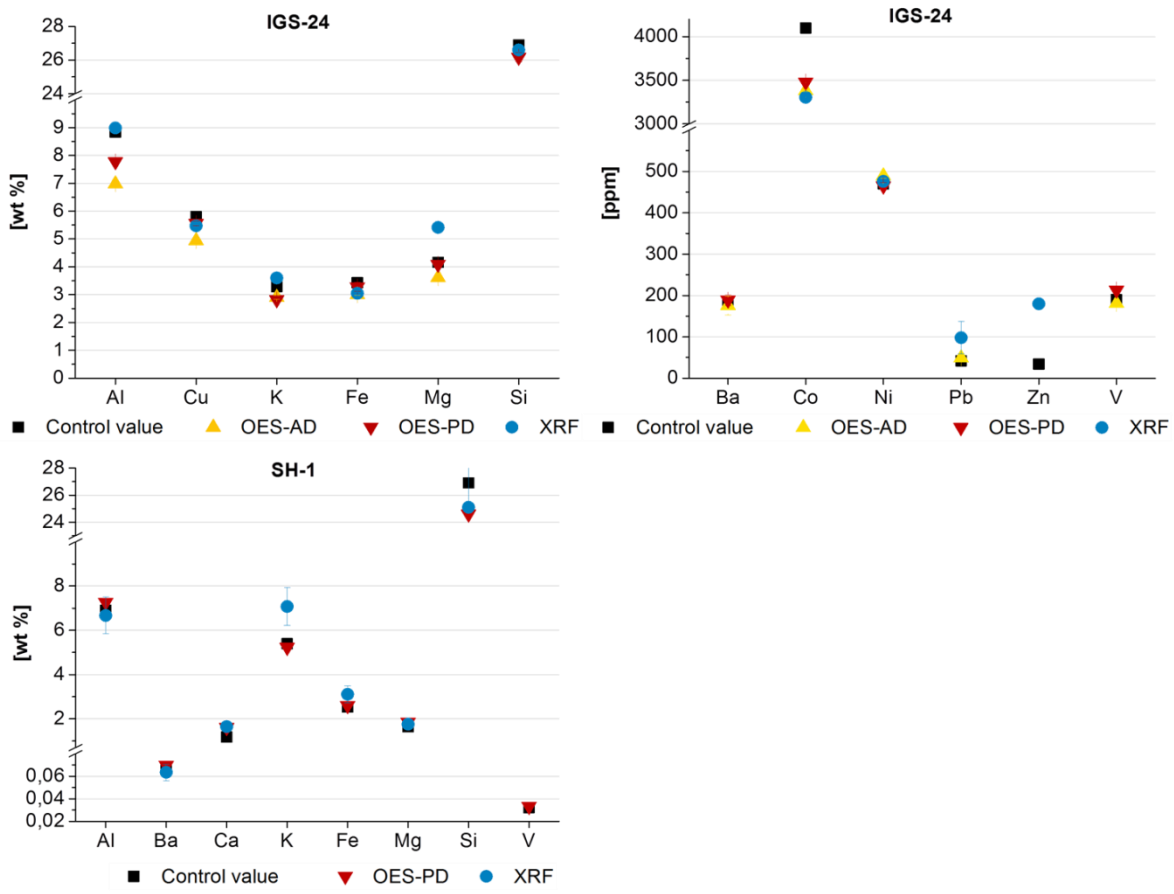

Figure 2: Illustration of element concentrations determined by OES-AD, OES-PD, and XRF in IGS-24 and SH-1

Assessment of analytical data

The number of elements contained in significant concentrations the Kupferschiefer and the number of methods used in this study does not allow a full presentation of the collected data. The complete data set can, however, be found in the electronic supplement. Data gathered by INAA serves as reference to judge the accuracy of the tested analytical techniques in the absence of a suitable reference material. The relative deviation of the analytical results to the ones determined by INAA is expressed in %. In most diagrams, the error bars of the INAA measurements are not visible since they usually range within 5 %.

263 This study illustrates the difficulties and pitfalls of various analytic methods suffering from the
264 Kupferschiefer black shale's complexity. An overview of technique-specific sources of error,
265 their occurrence and influence on the applied technique is given in table 4 and addressed
266 individually in the following section.

267
268 *Table 4: Overview of major sources of error in the measurements of different analytical*
269 *techniques*
270

Error source	OES-AD	OES-PD	XRF	TXRF
Pre-treatment	Low recuperation of Al, Cu, Co, Ni, Si, As, C_{org}	Incomplete digestion (Si, Al, Co, Ni) Loss of Ag	-	Digestion (see AD and PD)
Measurement	-	Matrix effects (Na) High detection limits	Matrix effects (sulfides)	Low energy resolution (full peak overlaps)
Processing	-	-	Correction with secondary data from CNS and XRD	Strong peak overlap (including internal standard)

271

272 *Base metal concentrations*

273 The Cu content was successfully measured in all samples using INAA. The copper concentration
274 was extrapolated from the ^{66}Cu isotope activity in samples taken from the pneumatic tube after
275 1-minute irradiation and generally about 6 to 15 minutes decay. ^{66}Cu was chosen for the
276 calculation of the Cu concentration based on the large peak to background ratio and high
277 neutron cross section. The samples carry diverse but overall high Cu concentrations ranging
278 from 0.6 to 26 wt% (Fig. 4). Measurements of Cu by ICP-OES, XRF, and TXRF show a large spread
279 of results (Fig. 4). The largest mismatch was found in TXRF data that underestimated the Cu
280 concentration in the Kupferschiefer samples vastly (ca. 37 % relative) compared to INAA data.

The XRF results deviate in individual measurements by a range of 2 to 25 % from INAA. While the results indicate clearly that high Cu concentrations are underestimated, low concentrations can also be overestimated (Fig. 3).

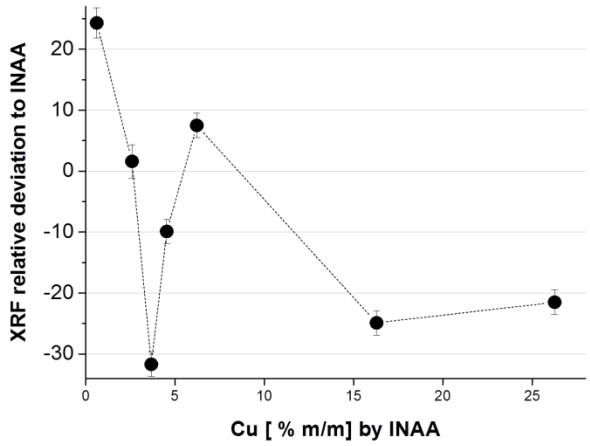

Figure 3: Relationship between Cu concentration determined by INAA and relative deviation of WD-XRF results

Best and most consistent results were delivered by ICP-OES analyses of AD and PD samples with a relative deviation from INAA results of only 5 %. About 5 % higher Cu concentrations were measured in PD samples compared to AD. Lower concentrations of Cu in AD samples are attributed to incomplete digestion of organic matter compared to PD. Systematic overestimation of Cu content due to the Na-rich PD solution by ICP-OES, could be disproven by the measurements of IGS-24 where instead only a minor underestimation by 4.1% was detected.

Zn concentrations range from tens of ppm to weight percent in the studied sample suite. The available Zn-INAA data supports the accuracy of OES results with an average deviation of only 7 % (Fig. 4). The average deviation of OES-AD from INAA is slightly increased relative to OES-PD due to the larger error associated with the measurement of smaller Zn concentrations. The Zn

detection limit of OES-AD and PD is below 30 ppm and 100 ppm, respectively. The primary cause for high detection limits associated with OES-PD appears to be the plasma condition that is directly influenced by the matrix components (Kragten and Parczewski, 1981; Olesik, 1991). Especially the addition of large quantities of Na to the flame increases the background in the ICP-OES continuum by recombination of ionized Na^+ and electrons (Olesik, 1991; Taylor, 2001; Hug, 2011; Harris, 2014, 2014). To circumvent this issue, a higher degree of dilution is required, lowering the detection limit (Hill, 2007), but also with the advantage of lowering the slightly increased viscosity in PD solutions caused by the high salt content. No clogging issues were observed in this study, but they can occur and should be considered (Boulyga et al., 2004).

Silicate-bound major element concentrations

Si cannot be measured in AD solutions, since it was expelled as H_2SiF_6/SiF_4 in the digestion process (Hill, 2007; Harris, 2014). ICP-OES results of peroxide digested samples appear to underestimate the Si content by an average of 5 % in relation to the values obtained from XRD, whereas a relative overestimation by 9 % is obtained by XRF (Fig. 4). These values are, however, well within the relative estimated error of 15 % of the XRD analysis. The same effect of Si underestimation by OES-PD was observed in the reference measurements SH-1 (-8.6 %) and to a minor degree in IGS-24 (-2.7 % deviation). This is most likely the result of incomplete dissolution of silicates during digestion (Heinrich and Hermann, 1990), despite a visually complete digestion with no noticeable residues or lack of clarity. The same effect is observed for Al with both OES-AD (relative deviation of 10 %) and PD (12 %), as well as in the reference sample IGS-24.

TXRF grossly underestimates the Si (28 %) and Al (36 %) concentration. The very variable element composition of Kupferschiefer samples is considered the most likely source for this systematic error. (Klockenkämper and Von Bohlen, 2015) describe in detail the capabilities of TXRF and discuss the limits of energy-dispersive spectroscopy by TXRF. Especially elements in the low energy region (< 10 keV) of EDS spectra (e.g. Al, Si, Fe, Co, Cu, among others) suffer from interferences. The probability of energy line interferences strongly increases in multi-element samples (Klockenkämper und Von Bohlen 2015). The error caused by overlapping peaks is often elevated in energy-dispersive systems in comparison to wavelength dispersive ones, despite the availability of correction programs (Jenkins, 1999). Furthermore, quantification of TXRF results depends strongly on the reliability of the internal standard and is based on a determination of net intensities in each spectrum. Bi and Y were the best possible internal standards, not contained in significant concentrations in the samples themselves. However, both still suffer from peak overlaps especially by Pb, which is contained in significant concentrations (up to 4.5 wt% measured by OES-AD) in the Kupferschiefer samples studied.

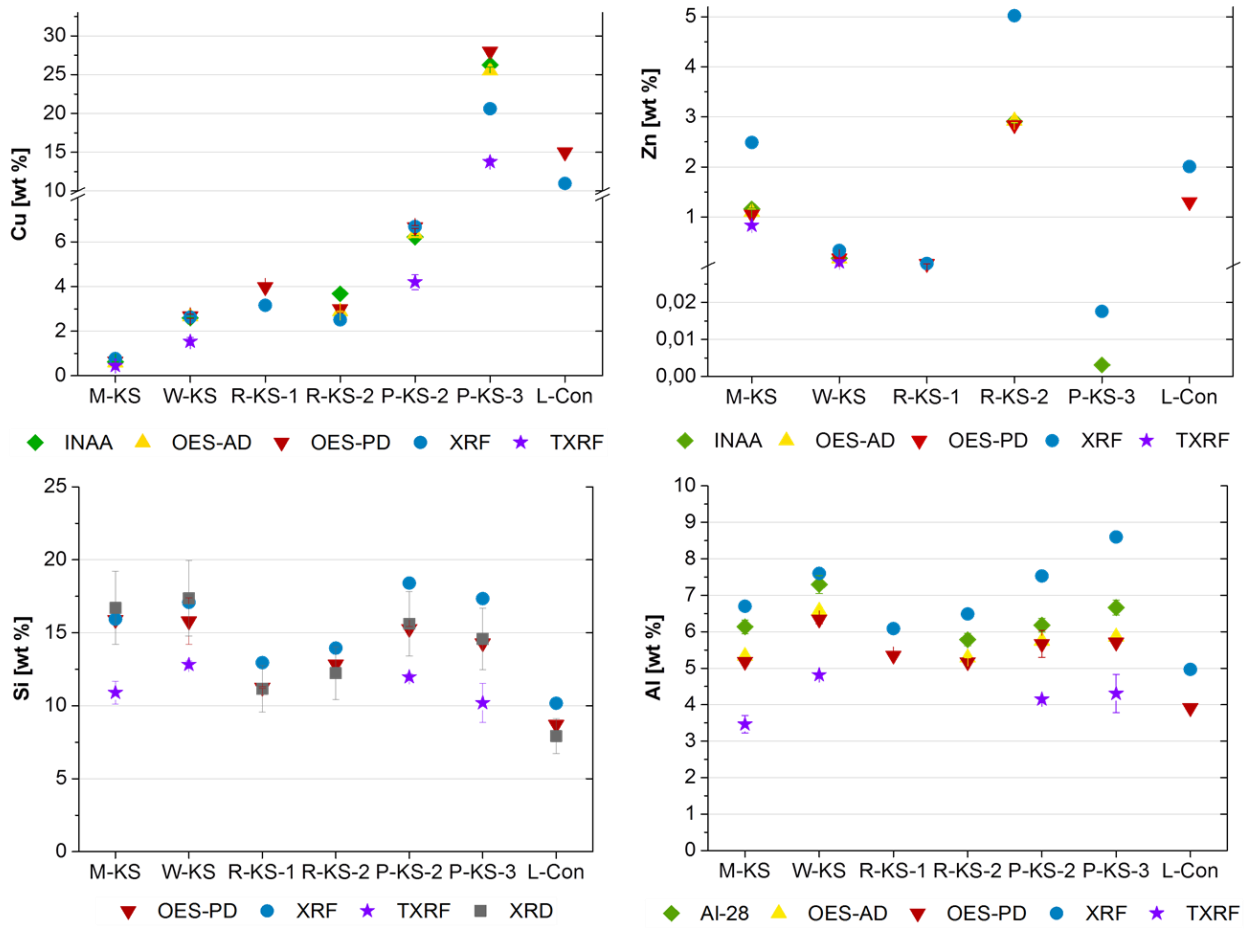

Figure 4: Illustration of Cu, Zn, Si and Al concentrations determined by INAA (Al from Al28), OES-PD/AD, XRF, TXRF, and XRD (based on calculation of Si content in quartz, sheet silicates and feldspars)

Trace element concentrations

While ICP-OES is commonly used to determine trace element concentrations, it is well known that one has to be cautious with XRF trace element results (Jenkins et al., 1995). The latter is supported by the rather erratic results received from the studied samples (Fig. 5). Generally, XRF overestimates Ag, As, Co, Ni, Mo and V by about 57 %, compared to INAA.

The best results for Ag were achieved with ICP-OES of AD samples. OES-AD Ag results deviate by ~15 % from the concentration determined by INAA and generally appear to underestimate the

Ag content. The measurement of silver in solution is known to be challenging due to the number of insoluble salts that can be formed (Joerger et al., 2000; Averill and Elderedge, 2006). Ag was expected to precipitate as chloride in the solution created by peroxide digestion because of the addition of hydrochloric acid. This assumption is supported by consistently lower Ag concentrations (about 12%) reported for PD samples analyzed by ICP-OES comparatively to AD measurement solutions. XRF overestimates the Ag content in all but those samples that are most enriched in Cu- and Ag (P-KS-03 and L-KS-Con), by an average of 22 % compared to INAA data. Ag was not determined by TXRF due to interferences caused by Ar within the ambient atmosphere (Klockenkämper and Von Bohlen, 2015).

OES-PD and INAA data on As are in good agreement. Deviation is greatest for OES-AD samples, where As is underestimated (W-KS). It is safe to assume that a major fraction of As is lost as volatile oxide during the AD digestion process – whereas it is evidently retained to a greater part during the PD process (Yu et al., 2001; Hill, 2007; Harris, 2014). The results may be further improved by the use of a lid during the caustic fusion. Low As concentrations could not be detected in PD samples due to a detection limit of 140 ppm.

Co is underestimated by XRF in contrast to other trace elements with the exception of the Cu-rich sample P-KS-3 where the Co concentration is grossly overestimated compared to INAA data. Co concentrations detected in PD and AD samples measured by OES are very similar to those determined by INAA with an average deviation of -8.5 %. Underestimation of Co was also found in IGS-24 and implies a higher resistance of Co to digestion.

OES-AD and PD results for Mo match closely (~3 % deviation). They deviate by about ~11 % from the values determined by INAA, but remain in most cases within the high uncertainty of INAA

368 for Mo. The concentrations measured by XRF are much higher, except in sample P-KS-3 (Fig. 5).
369 The XRF analysis of Mo, Co, and Ni, but also Al, and Si appears to be influenced by the
370 abundance of Cu (eg. P-KS-3, Fig. 4, 5), resulting in over- or underestimation of the respective
371 trace element concentrations. These observations are most likely influenced by matrix effects in
372 the pressed pellets. Such effects have been observed by a number of authors (Spangenberg et
373 al., 1994; Sieber, 2002). While the absorption contrast between the lighter (Si, Al) and heavier
374 elements (Cu, Pb, Zn) is a source of concern, more so are element interactions causing
375 secondary absorption and enhancement reactions (Mainardi et al., 1982; Jenkins et al., 1995;
376 Jenkins, 1999). In extreme cases, secondary fluorescence causing enhancement can account for
377 50% observed emissions (Tertian, 1982).
378 V concentrations measured by XRF closely match the ones determined by INAA, with only a
379 slight average deviation of about 4.9%. ICP-OES detected in all samples considerably lower V
380 concentrations with average deviation of 23 % from the concentrations determined with INAA.
381

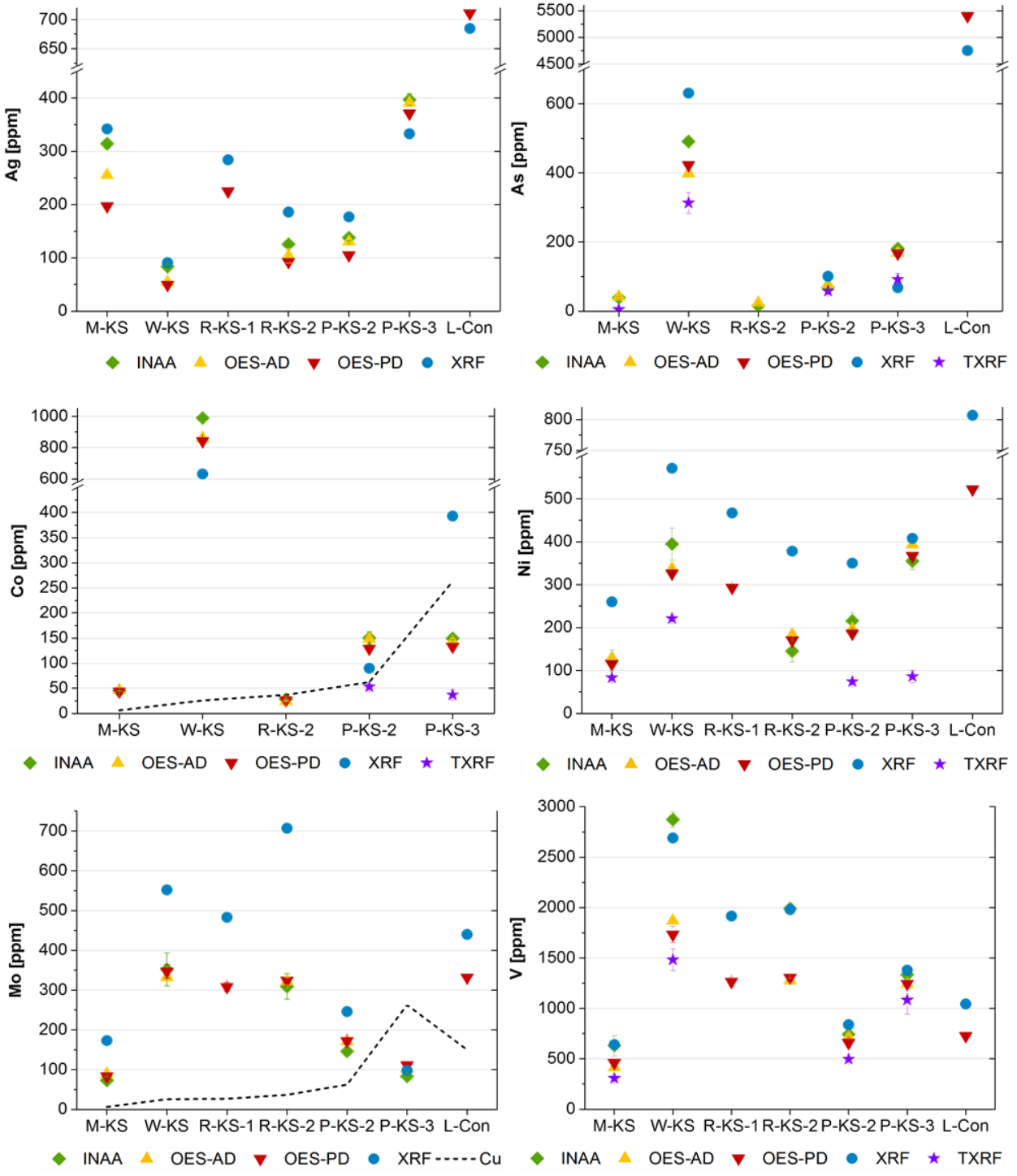

382

383 *Figure 5: Illustration of trace element (Ag, As, Co, Mo, Ni, V) concentrations determined by INAA,*
384 *OES-PD, XRF, and TXRF. The dotted line marks the relative copper concentration within the*
385 *samples based on INAA*
386

387

Assessment of analytical techniques

ICP-OES

A comparison of the results collected with ICP-OES and INAA show a high accuracy for the base metals Co, Cu, Ni, Mo, Zn (Fig. 6) as well as for Si and Al. Variations are larger and less consistent for other elements. The volatile As was determined with a relatively high accuracy by OES-PD but deviated stronger in OES-AD measurements. The opposite was observed for Ag. The measurements itself possess a low relative standard deviation (RSD) of less than 0.5 and 5 % at concentrations above and below 1000 ppm respectably.

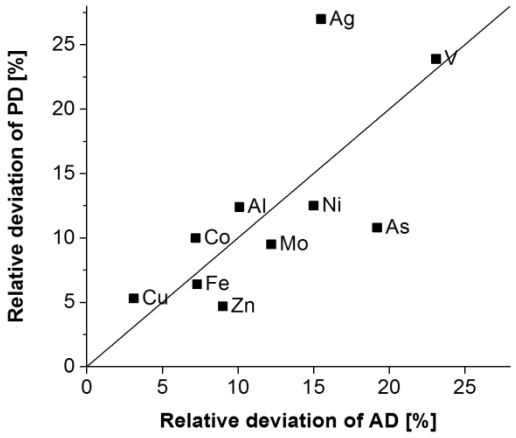

Figure 6: Relative average deviation of OES-AD and PD measurements from INAA

In summary it can be said, that both digestion procedures are associated with a lower accuracy than is normally acceptable for ICP-OES, but deliver sufficiently accurate data (if one assumes that an error of below ~15 % relative to INAA is acceptable). Acid digestion allows for a more accurate determination of the silver content but requires the use of hazardous chemicals like HF, especially trained personal, and more time. Sample preparation by PD is much more rapid (10-20 minutes/sample), facilitating a higher sample throughput. This technique can additionally

405 retain higher concentration of volatiles and offers a complete digestion associated with a
406 slightly increased copper concentration. A serious disadvantage is the composition of the
407 matrix, which leads to high detection limits.
408
409 *WD-XRF*
410 WD-XRF measurements of pressed pellets had to be preceded by XRD and TC measurements to
411 determine the type of oxide and sulfide compounds contained in the sample in addition to the
412 total carbon content, increasing the necessary time required for analysis compared to ICP-OES.
413 The results obtained for the light elements (Si and Al) have a high but acceptable deviation of
414 about 15 % for Si and Al compared to the XRD and INAA data. The erratic, often overestimated
415 As, Co, Ni, Mo, Zn and underestimated Cu, Co concentrations, in comparison to results collected
416 by INAA and ICP-OES, are unsatisfactory. Therefore it appears to be advisable to avoid any base
417 metal and trace element measurements in Kupferschiefer by XRF.
418 The results gained with XRF on pressed pellets are not unexpected. They have clear
419 repercussions on the established operative mode to quantify base metal concentrations in
420 Kupferschiefer with XRF-based techniques. Fused glass beads are an alternative option to avoid
421 negative effects associated with pressed pellets. However, established sample preparation
422 procedures cannot be used and a suitable calibration program must be developed to recalculate
423 the original composition of the oxidized sample. A complete oxidation of the sample cannot be
424 achieved by calcination since the sintered material is impossible to remove from any crucible.
425 The subsequent fusion-step within a Pt-crucible using lithium-tetraborate flux should not be
426 attempted due to the composition of the sample material and possible destruction of the Pt-

crucible (Bennett and Oliver, 1992; Jenkins et al., 1995; Lupton et al., 1997; Harris, 2014). Kupferschiefer is very reducing and rich in copper, arsenic, silicon and organic carbon. All of these substances are known as platinum poisons that will cause structural disintegration of the platinum crucible (Lupton et al., 1997). Zirconium crucibles were tested as a possible alternative to platinum. They are not affected by the platinum toxins; however, tests showed that their heat conductivity is insufficient to achieve complete fusion. Studies focusing on the analysis of sulfide ores suggest two alternative approaches to fusion (Petin et al., 1985; Loubser and Verryn, 2008), but have not yet been verified by other authors.

TXRF

Analysis of Kupferschiefer suspensions by TXRF did not yield any useful results. All detected elements were vastly underestimated by -20 to -50 % relative to INAA data. This effect could also be observed in trial analysis of AD and PD solutions by TXRF, which resulted in similar underestimation of element concentrations. Sample preparation itself appears therefore to only affect the detection limits but not influence on the accuracy of the data (Klockenkämper and Von Bohlen, 2015). The usefulness of TXRF in bulk geochemical analysis of Kupferschiefer is further limited by the lack of Mo and Ag data and can therefore not be recommended. The same is to be considered for other energy-dispersive XRF measurement systems.

Conclusions

A critical assessment of several analytical methods for the bulk analysis of the geochemical composition of mineralized Kupferschiefer illustrates that ICP-OES yields robust data whilst at

the same time requiring for a simple and efficient sample preparation process. Nevertheless, relative deviations relative to INAA reference data were still in the range of 5 to 20 %. Measurements of acid digested (AD) solutions showed overall results with a higher accuracy but slightly lower Cu concentrations as compared to Na-peroxide digested (PD) solutions. Na-peroxide digested solutions carry the advantages of a much faster sample preparation and complete digestion. However, these advantages are offset by losses in Ag and higher detection limits.

In accordance with the results, both acid and peroxide digestion with subsequent ICP-OES analysis can be recommended for the analysis of Kupferschiefer (Fig. 7). Whilst ICP-OES measurements and the sample preparation through digestion are more time consuming compared to the ones used for XRF, the data quality is better and there is no explicit requirement for additional TC data, mineralogical measurements or data correction. Nonetheless, additional mineralogical data (XRD) or knowledge about the TOC content (CNS) are recommended to be collected to fully understand the material and identify potential errors.

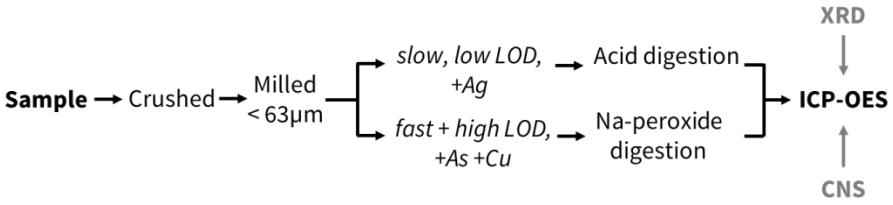

Figure 7: Recommended flow chart for the multi-element analysis of Kupferschiefer (LOD: limit of detection)

For future work there is a vital need for a Kupferschiefer reference material that represents the complexities of base metal sulfides closely associated with abundant organic matter, with silicate and carbonate minerals. Availability of such a standard would allow a direct and precise

comparison of results generated in different laboratories and to estimate and trace potential discrepancies.

Acknowledgements

We would like to convey our thanks to Dany Savard (Universite du Quebec a Chicoutimi) for providing us access to the SH-1 black shale in-house standard and for discussing analytical problems. Further thank goes to Thurit Tschöpe (TUBAF) for handling the challenging ICP-OES measurements of peroxide solutions and Rahel Bertheau for testing TXRF measurements on the digested sample solutions. CNS data and milled Kupferschiefer sample R-KS-1 were kindly provided by Juliane Schäfer of the UVR-FIA (Germany). The authors would also like to thank KGHM Polska Miedź S.A. and KGHM Cuprum who provided access and provision of the concentrate sample. This work was part of the EcoMetals project and was financially supported by the German Ministry of Education and Research BMBF (Ref. Nr. 033RF001).

References

Averill, B.A. and Elderedge, P. (2006) *Chemistry: Principles, Patterns, Applications,* Prentice Hall.

Axios SuperQ Reference Manual, 2005.

Balcerzak, M. (2002) Sample digestion methods for the determination of traces of precious metals by spectrometric techniques. Analytical Sciences, 18, 737–750.

Bechtel, A., Ghazi, A.M., Elliott, W.C. and Oszczepalski, S. (2001a) The occurrences of the rare earth elements and the platinum group elements in relation to base metal zoning in the vicinity of Rote Fäule in the Kupferschiefer of Poland. Applied Geochemistry, 16, 375–386.

Bechtel, A., Gratzer, R., Püttmann, W. and Oszczepalski, S. (2001b) Variable alteration of organic matter in relation to metal zoning at the Rote Fäule front (Lubin-Sieroszowice mining district, SW Poland). Organic Geochemistry, 32, 377–395.

Bechtel, A., Gratzer, R., Püttmann, W. and Oszczepalski, S. (2002) Geochemical characteristics across the oxic/anoxic interface (Rote Fäule front) within the Kupferschiefer of the Lubin-Sieroszowice mining district (SW Poland). Chemical Geology, 185, 9–31.

Bechtel, A., Shieh, Y.-N., Elliott, W.C., Oszczepalski, S. and Hoernes, S. (2000) Mineralogy, crystallinity and stable isotopic composition of illitic clays within the Polish Zechstein basin: implications for the genesis of Kupferschiefer mineralization. Chemical Geology, 163, 189–205.

Bennett, H. and Oliver, G. (1992) *XRF Analysis of Ceramics, Minerals and Allied Materials,* Wiley, Chichester.

Borg, G., Frotzscher, M. and Ehling, B. (2005) Metal content and spatial distribution of Au and PGE in the Kupferschiefer of the Mansfeld/Sangerhausen mining district, Germany. In *Mineral Deposit Research: Meeting the Global Challenge*, pp. 885–888.

Borg, G., Piestrzynski, A., Bachmann, G.H., Püttmann, W., Walther, S. and Fiedler, M. (2012) An Overview of the European Kupferschiefer Deposits. Economic Geology Special Publication, 16, 455–486.

Boulyga, S.F., Pickhardt, C. and Becker, J.S. (2004) New approach of solution-based calibration in laser ablation inductively coupled plasma mass spectrometry of trace elements in metals and reduction of fractionation effects. Atomic Spectroscopy, 25, 53–101.

Halicz, L. and Russell, G.M. (1986) Simultaneous determination, by hydride generation and inductively coupled plasma atomic emission spectrometry, of arsenic, antimony, selenium and tellurium in silicate rocks containing the noble metals and in sulphide ores. Analyst, 111, 15–18.

Harris, D.C. (2014) *Lehrbuch der Quantitativen Analyse,* 8th edn., Springer Spektrum, Berlin Heidelberg.

Heinrich, H. and Hermann, A.G. (1990) *Praktikum der Analytischen Geochemie,* Springer-Lehrbuch, Berlin.

Henrique-Pinto, R., Barnes, S.-J., Savard, D.D. and Mehdi, S. (2017) Quantification of metals and semi-metals in carbon-rich rocks: A new sequential protocol including extraction of humic substances. Geostandards and Geoanalytical Research, 41, 41–62.

Hill, S.J. (2007) *Inductively Coupled Plasma Spectrometry and its Applications,* Blackwell, Oxford.

Hug, H. (2011) *Instrumentele Analytik*: *Theorie und Praxis,* 2nd edn., Europa-Lehrmittel, Haan-Gruiten.

Jenkins, R. (1999) *X-Ray Fluorescence Spectrometry,* Chemical analysis: A series of monographs on analytical chemistry and its applications Volume 152, Wiley, New York.

Jenkins, R., Gould, R.W. and Gedcke, D. (1995) *Quantitative X-ray Spectrometry,* Practical Spectroscopy Series 20, Dekker, New York.

Joerger, R., Klaus, T., Petterson, J. and Granqvist, C.G. (2000) Digestion method for silver accumulated in micro-organisms. Fresenius Journal of Analytical Chemistry, 366, 311–312.

Kamradt, A., Borg, G., Schaefer, J., Kruse, S., Fiedler, M., Romm, P., Schippers, A., Gorny, R., du Bois, M., Bieligk, C., Liebetrau, N., Nell, S., Friedrich, B., Morgenroth, H., Wotruba, H. and Merkel, C. (2012) An Integrated Process for Innovative Extraction of Metals from Kupferschiefer Mine Dumps, Germany. Chemie Ingenieur Technik, 84, 1694–1703.

Kane, J.S., Arbogast, B. and Leventhal, J. (1990) Characterization of Devonian Ohio shale SDO-1 as a USGS geochemical reference sample. Geostandards Newsletter, 14, 169–196.

KGHM Polska Miedź (2015) *Mineral resources and reserves report*: *as at December 31, 2014*.

Klockenkämper, R. and Von Bohlen, A. (2015) *Total-reflection X-ray fluorescence analysis and related methods*: *Second Edition,* Chemical analysis: A series of monographs on analytical chemistry and its applications 181, Wiley, New York.

Kragten, J. and Parczewski, A. (1981) Factorial analysis of matrix effects in ICP-OES and AAS Determination of Ta and Ni IN Au. Talanta, 28, 901–907.

538 Kutschke, S., Guézennec, A.G., Hedrich, S., Schippers, A., Borg, G., Kamradt, A., Gouin, J., Giebner, F.,
539 Schopf, S., Schlömann, M., Rahfeld, A., Gutzmer, J., D'Hugues, P., Pollmann, K., Dirlich, S. and
540 Bodénan, F. (2015) Bioleaching of Kupferschiefer blackshale – A review including perspectives of the
541 Ecometals project. Minerals Engineering, 75, 116–125.
542 Lister, B. (1978) The Preparation of Twenty Ore Standards, IGS 2O-39. Preliminary Work and Assessment
543 Of Analytical Data. Geostandards Newsletter, 2, 157–186.
544 Loubser, M. and Verryn, S. (2008) Combining XRF and XRD analyses and sample preparation to solve
545 mineralogical problems. South African Journal of Geology, 111, 229–239.
546 Lupton, D.F., Merker, J. and Schölz, F. (1997) The Correct Use of Platinum in the XRF Laboratory. X-ray
547 Spectrometry, 26, 132–140.
548 Mainardi, R.T., Fernandez, J.E. and Nores, M. (1982) Influence of interelement effects on x-ray
549 fluorescence calibration curve coefficients for binary mixtures. X-ray Spectrometry, 11, 70–78.
550 Matlakowska, R. and Sklodowska, A. (2011) Biodegradation of Kupferschiefer black shale organic matter
551 (Fore-Sudetic Monocline, Poland) by indigenous microorganisms. Chemosphere, 9, 1255–1261.
552 Matlakowska, R., Sklodowska, A. and Nejbert, K. (2012) Bioweathering of Kupferschiefer black shale
553 (Fore-Sudetic Monocline, SW Poland) by indigenous bacteria: implication for dissolution and
554 precipitation of minerals in deep underground mine. FEMS Microbiology Ecology, 81, 99–110.
555 Müller, N., Franke, K., Schreck, P., Hirsch, D. and Kupsch, H. (2008) Georadiochemical evidence to
556 weathering of mining residues of the Mansfeld mining district, Germany. Environmental Geology, 54,
557 869–877.
558 NIST *National Institute of Standards and Technology, U.S.*
559 Olesik, J.W. (1991) Elemental analysis using ICP-OES and ICP/MS: An evaluation and assessment of
560 remaining problems. American Chemical Society, 63, 12–21.
561 Oszczepalski, S., Speczik, S. and Wojciechowski, A. (2011) Gold mineralization in the Kupferschiefer
562 oxidized series of the North Sudetic trough, SW Poland. Gold in Poland, AM Monograph, 2, 153–168.
563 Paul, J. (2006) The Kupferschiefer: Lithology, stratigraphy, facies and metallogeny of a black-shale.
564 Zeitschriften der Deutschen Gesellschaft für Geowissenschaften, 157, 57–76.
565 Pertov, L.L., Kornakov, Y.N., Korotaeva, I.I., Anchutina, E.A., Persikova, L.A., Susloparova, V.E., Fedorova,
566 I.N. and Shibanov, V.A. (2007) Multi-element reference samples of black shale. Geostandards and
567 Geoanalytical Research, 89–102.
568 Petin, J., Wagner, A. and Bentz, F. (1985) Combination of oxidation and melt treatment for a rapid
569 preparation of metallic and other oxidizing samples for X-ray fluorescence analysis. Steel research,
570 56, 215–218.
571 Piestrzynski, A. and Pieczonka, J. (2012) Low temperature ore minerals associations in the Kupferschiefer
572 type deposit, Lubin-Sieroszowice Mining District, SW Poland. Mineralogical Review, 62, 59–66.
573 Quinby-Hunt, M.S., Wilde, P., Orth, C.J. and Berry, W.B. (1989) Elemental geochemistry of black shales -
574 Statistical comparison of low-calcic shales with other shales. U. S. Geological Circular, 1037
575 Metalliferous Black Shales and Related Deposits, 8–15.
576 Rahfeld, A., Kleeberg, R., Möckel, R. and Gutzmer, J. (submitted 2017) Quantitative mineralogical analysis
577 of the European Kupferschiefer. Minerals Engineering.

578 Schubert, M., Morgenstern, P., Wennrich, R., Freyer, K. and Weiss, H. (2003) The weathering behavior of
579 heavy metals in ore processing residues (Mansfeld region, Germany). Mine Water and the
580 Environment, 22, 2–6.
581 Sieber, J.R. (2002) Matrix-independent XRF methods for certification of standard reference materials.
582 Advances in X-ray Analysis, 45, 493–504.
583 Spangenberg, J., Fontbote, L. and Pernicka, E. (1994) X-Ray fluorescence analysis of base metal sulphide
584 and iron–manganese oxide ore samples in fused glass disc. X-ray Spectrometry, 23, 83–90.
585 Speczik, S. (1995) The Kupferschiefer mineralization of Central Europe: New aspects and major areas of
586 future research. Ore Geology Reviews, 9, 411–426.
587 Sun, Y. and Püttmann, W. (2004) Composition of kerogen in Kupferschiefer from southwest Poland.
588 Chinese Journal of Geochemistry, 23, 101–111.
589 Taylor, H.E. (2001) *Inductively Coupled Plasma-Mass Spectrometry*: *Practices and Techniques,* Academic
590 Press, San Diego.
591 Tertian, R. (1982) *Principles of Quantitative X-ray Fluorescence Analysis,* 1st edn., Heyden, London.
592 Thomson Reuters (ed.) (2015) *GFMS Annual Survey*.
593 Twyman, R.M. (2005) Sample dissolution for elemental analysis: Wet digestion. In *Encyclopedia of*
594 *Analytical Science (Second Edition)*, eds. P. Worsfold, A. Townshend and C. Poole. Elsevier Science,
595 London UK, 8, pp. 146–153.
596 Vaughan, D.J., Sweeney, M.A., Friedrich, G., Diedel, R. and Haranczyk, C. (1989) The Kupferschiefer; an
597 overview with an appraisal of the different types of mineralization. Economic Geology, 84, 1003–
598 1027.
599 Wedepohl, K.H. (1964) Untersuchungen am Kupferschiefer in Nordwestdeutschland; Ein Beitrag zur
600 Deutung der Genese bituminöser Sedimente. Geochimica et Cosmochimica Acta, 28, 305–364.
601 Wennrich, R., Niebergall, K., Zwanziger, H. and Just, G. (1988) Geochemische Untersuchungen an
602 Kupferschiefer mittels INAA und quantitative Multielement-Verteilungsanalyse am geologischen
603 Kompaktmaterial unter Verwendung der Laser - ICP - AES. Isotopenpraxis, 24, 97–106.
604 Westphal, G.P. (2008) Review of loss-free counting in nuclear spectroscopy. Journal of Radioanalytical
605 and Nuclear Chemistry, 275, 677–685.
606 Yu, Z., Robinson, P. and McGoldrick, P. (2001) An Evaluation of Methods for the Chemical Decomposition
607 of Geological Materials for Trace Element Determination using ICP-MS. Geostandards and
608 Geoanalytical Research, 25, 199–217.